NeuroImage: Clinical 21 (2019) 101671

Contents lists available at ScienceDirect

NeuroImage: Clinical

journal homepage: www.elsevier.com/locate/ynicl

# Nuclei-specific thalamic connectivity predicts seizure frequency in drug-resistant medial temporal lobe epilepsy

Hang Joon Jo[a,b,c,*], Daniel L. Kenny-Jung[a], Irena Balzekas[a], Eduardo E. Benarroch[a], David T. Jones[a,c], Benjamin H. Brinkmann[a,d], S. Matt Stead[a], Jamie J. Van Gompel[b], Kirk M. Welker[c], Gregory A. Worrell[a,*]

[a] Department of Neurology, Mayo Clinic, Rochester, MN 55905, USA
[b] Department of Neurologic Surgery, Mayo Clinic, Rochester, MN 55905, USA
[c] Department of Radiology, Mayo Clinic, Rochester, MN 55905, USA
[d] Department of Biomedical Engineering and Physiology, Mayo Clinic, Rochester, MN 55905, USA

A B S T R A C T

*Background and objectives:* We assessed correlations between the resting state functional connectivity (RSFC) of different thalamic nuclei and seizure frequency in patients with drug-resistant medial temporal lobe epilepsy (mTLE).
*Methods:* Seventeen patients with mTLE and 17 sex-/age-/handedness-matched controls participated. A seed-based correlation method for the resting-state FMRI data was implemented to get RSFC maps of 70 thalamic nuclei seed masks. Group statistics for individual RSFC for subjects and seed masks were performed to obtain within-group characteristics and between-group differences with age covariates. A linear regression was applied to test whether seizure frequency correlated with thalamic nuclear RSFC with the whole brain in mTLE patients.
*Results:* RSFC of thalamic nuclei showed spatially distinguishable connectivity patterns that reflected principal inputs and outputs that were derived from priori anatomical knowledge. We found group differences between normal control and mTLE groups in RSFC for nuclei seeds located in various subdivisions of thalamus. The RSFCs in some of those nuclei were strongly correlated with seizure frequency.
*Conclusions:* Mediodorsal thalamic nuclei may play important roles in seizure activity or in the regulation of neuronal activity in the limbic system. The RSFC of motor- and sensory-relay nuclei may help elucidate sensory-motor deficits associated with chronic seizure activity. RSFC of the pulvinar nuclei of the thalamus could also be a key reflection of symptom-related functional deficits in mTLE.

## 1. Introduction

Mesial temporal lobe epilepsy (mTLE) is frequently resistant to pharmacological treatment, with a large proportion of mTLE patients experiencing uncontrolled seizures and/or drug-related adverse effects (Kwan and Brodie, 2000). Resective surgery can be curative for refractory mTLE, but it is often not an option due to bilateral disease or a focus involving the dominant temporal lobe (Gloor et al., 1982; Wiebe et al., 2001). For such cases, thalamic neurostimulation has been shown to be a useful therapeutic option (Bergey et al., 2015).

The thalamus is a complex structure containing multiple nuclei with specific functional roles as relays or processing hubs of neural signals between brain structures, including subcortical regions, the hippocampus and cortical areas (Jones, 2007; Kumar et al., 2017). Given the well-known and multifaceted role of the thalamus in epilepsy (Tasker et al., 1982; Velasco et al., 1987), it is not surprising that therapies targeting the thalamus have been successful in patients with refractory epilepsy. Deep brain stimulation (DBS) of the anterior nucleus of the thalamus is in wide clinical use, with some data pointing to possible mechanisms of action (Boon et al., 2007; Cukiert et al., 2017; Salanova et al., 2015).

While stimulation of specific thalamic nuclei is promising, advancement in the field has been hampered by knowledge gaps and the limited accessibility of the thalamus due to its deep location. Much of what is known about the anatomy and connectivity of the thalamus has come from pathology or animal studies (den Heijer et al., 2018; Gill et al., 2017; Warren et al., 2017). Advances in neuroimaging promise to deliver an improved understanding of thalamic connectivity in epilepsy (Barron et al., 2015; Barron et al., 2014). Although connectivity of the thalamus has been characterized using methods such as resting state functional magnetic resonance imaging (FMRI), it is only recently that thalamic connectivity has been assessed on the level of individual thalamic nuclei.

Further understanding of the thalamus in epilepsy and the therapeutic effects of thalamic stimulation has been limited by our understanding of the normal connectivity of this small and complex structure.

* Corresponding authors at: 200 First Street SW, Rochester, MN 55905, USA.
*E-mail addresses:* Jo.Hang@mayo.edu (H.J. Jo), Worrell.Gregory@mayo.edu (G.A. Worrell).

https://doi.org/10.1016/j.nicl.2019.101671
Received 6 September 2018; Received in revised form 31 December 2018; Accepted 7 January 2019
Available online 09 January 2019

Much of what is known about the anatomy and connectivity of the thalamus has come from disease models, animal studies, or studies considering all of the thalamic nuclei as a whole (den Heijer et al., 2018; Gill et al., 2017; Warren et al., 2017). It is only recently that thalamic connectivity has been assessed on the level of individual thalamic nuclei in human imaging studies of healthy subjects. With multiple strategies published for segmentation of individual nuclei within the thalamus (Battistella et al., 2017; Zhang and Li, 2017), diffusion MRI has now been used to delineate thalamic nuclei and the cortical networks to which they project (Lambert et al., 2017). Advances in nucleus-specific imaging promise to improve our current understanding of thalamic functional connectivity (FC) in epilepsy (Barron et al., 2015; Barron et al., 2014).

In this study, we present functional connectivity (FC) between the cortex and specific thalamic nuclei in control subjects and in patients with mTLE. We further demonstrate correlations between functional connectivity and seizure frequency.

## 2. Methods

### 2.1. Subject recruitment, assessment and ascertainment of clinical scores

All participants provided written informed consent in accordance with research protocols approved by the institutional review board of Mayo Clinic. Subjects were evaluated for drug-resistant epilepsy and underwent a clinical 3T seizure protocol MRI, which included T1-weighted MPRAGE, double inversion recovery, T2-weighted FLAIR, and diffusion weighted sequences.

A comprehensive evaluation, which included diagnostics, screening, seizure recordings, and epilepsy localization, yielded 17 patients with mTLE that fit study criteria (Table 1). There is no thalamic atrophy found in structural images by the visual inspection of board-certified neuroradiologists. Seventeen healthy control subjects were matched to the mTLE subjects by age, gender, and handedness. All control subjects were free of neurological disease.

### 2.2. MRI acquisition

Anatomical and functional MRI images were acquired in all subjects on a Siemens 3 T Magnetom Skyra system using a commercial 32-channel array head coil and tetrahedron-shaped foam pads to minimize head movement, prior to invasive electroencephalogram (EEG) recordings for precise diagnosis and epilepsy localization. High-resolution structural whole-brain images were acquired using a T1-weighted MPRAGE sequence with $0.5 \times 0.5 \times 1.2\,mm^3$ resolution, TR = 2.3 s, TI = 0.9 s, TE = 1.96 ms, and FA = 9°, identical to the clinical sequence. Subjects were instructed to open their eyes while resting state (RS) FMRI data were acquired with a gradient echo-planar sequence sensitive to blood oxygenation level–dependent contrast with $3.2 \times 3.2 \times 3.3\,mm^3$ resolution, 50 slices, TR = 2.9 s, TE = 30 ms, FA = 90°, and total acquisition time of 464 s (160 TRs).

### 2.3. Preprocessing of imaging data

Preprocessing of all imaging data was conducted using the Analysis of Functional NeuroImages (AFNI) software package (Cox, 1996). The first four volumes from each RS FMRI dataset were removed, and the effects of cardiac and respiratory disturbances were corrected by adaptive cyclic physiologic noise modeling (Beall, 2010). The time series of RS FMRI data were despiked, and then corrected for slice time acquisition differences and head motion. The remaining effects of noise signals including head-motion inferences (12 regressors; 3 translation, 3 rotation parameters, and their first derivatives), non-gray matter signals (4 regressors; 2 averaged timeseries from eroded lateral ventricle masks, and their first derivatives), and hardware-related artifacts (1 localized regressor from eroded white matter mask) were also corrected by the anatomy-based image correction method (Jo et al., 2010). Subsequently, spatial smoothing with an isotropic Gaussian kernel (full-width-at-half-maximum = 4 mm) was applied to the residual time series. The image volumes with inter-TR motion over 0.3 mm were censored to suppress bias from head motion in subsequent RSFC analysis (Jo et al., 2013). Using the robust non-linear warping function (3dQWarp) of the AFNI package, all image data were registered to the T1 atlas brain of the Montreal Neurological Institute and linearly resampled in the 1 mm isocubic grid space. The registration results for the image data of all subjects were visually inspected for subcortical and cortical brain structures.

**Table 1**
Demographic information for subjects with temporal lobe epilepsy (TLE). Normal control subjects were matched for age, sex, and handedness ($N = 17$, mean age difference = 0.63; $p = .84$).

| Subject index (N = 17) | Seizure foci observed by video/EEG | | Gender | Handedness | Age (years) | Epilepsy duration (years) | Seizure frequency (last 3 months) | Significant structural abnormality observed in MRI |
|---|---|---|---|---|---|---|---|---|
| | Left temporal ($n = 14$) | Right temporal ($n = 8$) | | | | | | |
| 01 | T | T | Female | Right | 29 | 7 | 0.5 | None |
| 02 | | T | Female | Right | 62 | 50 | 0.1 | None |
| 03 | T | | Male | Right | 35 | 16 | 8 | None |
| 04 | T | | Female | Right | 43 | 42 | 8 | None |
| 05 | | T | Male | Right | 29 | 28 | 30 | Right mesial temporal sclerosis |
| 06 | T | T | Female | Right | 38 | 2 | 1 | None |
| 07 | T | | Female | Right | 19 | 16 | 4 | None |
| 08 | T | | Male | Right | 33 | 32 | 24 | Left hippocampal atrophy |
| 09 | T | | Male | Right | 21 | 12 | 3 | None |
| 10 | T | T | Female | Right | 25 | 4 | 30 | None |
| 11 | T | | Male | Left | 20 | 7 | 2 | None |
| 12 | T | | Male | Right | 29 | 1 | 20 | None |
| 13 | | T | Female | Right | 53 | 2 | 3 | Right temporal encephalocele |
| 14 | T | T | Male | Right | 61 | 9 | 4 | Bilateral hippocampal volume loss |
| 15 | T | | Female | Right | 23 | 22 | 1 | Left hippocampal atrophy |
| 16 | T | | Female | Left | 35 | 6 | 16 | None |
| 17 | T | T | Female | Right | 45 | 3 | 24 | Minimal chronic ischemic/degenerative changes in subcortical white matter of both frontal lobes |

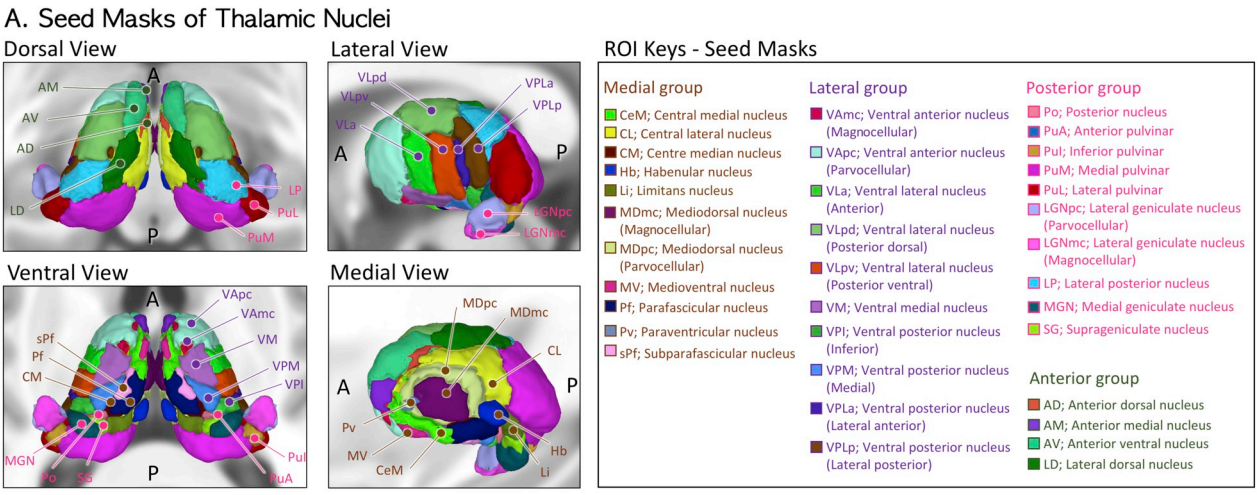


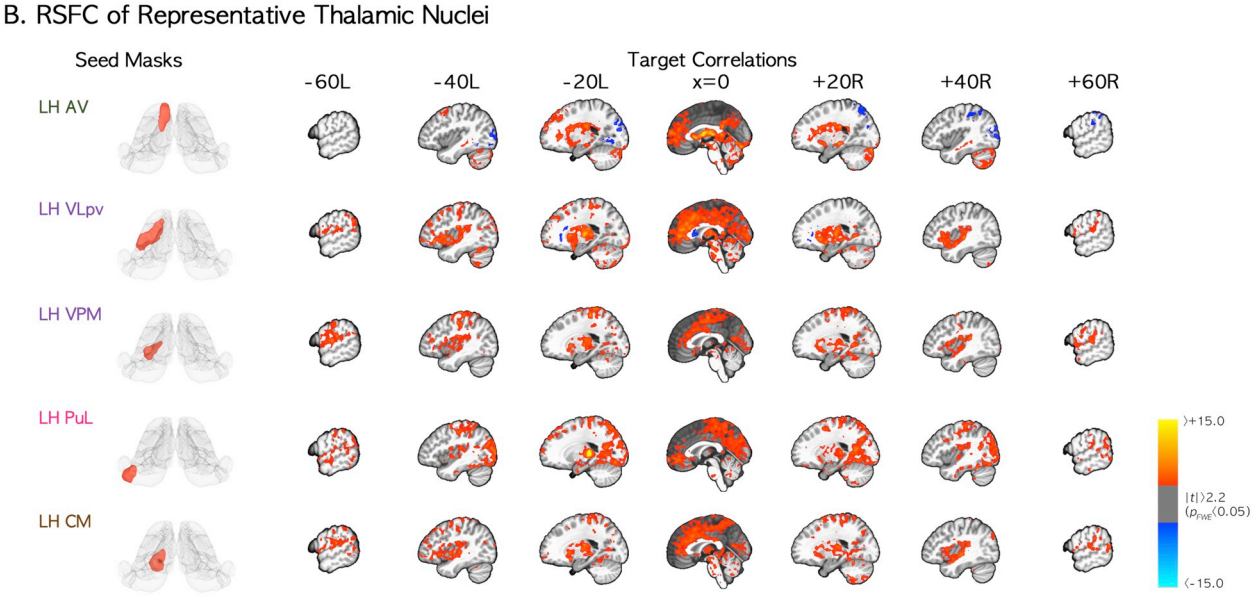


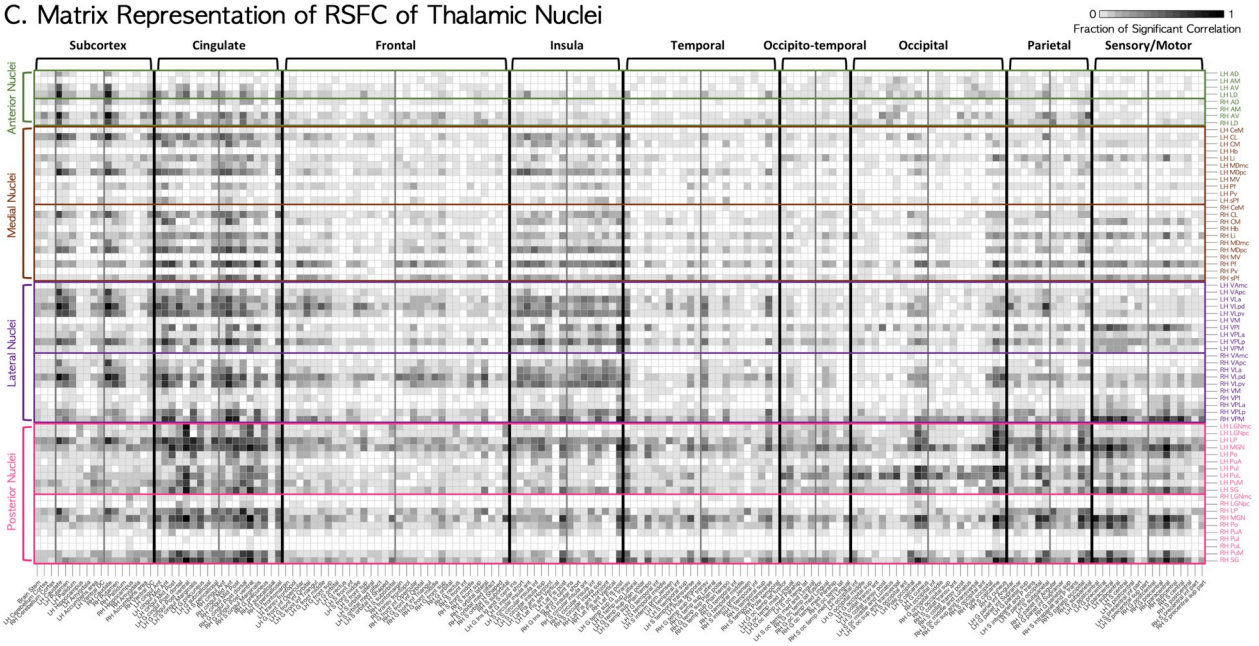


*(caption on next page)*

**Fig. 1.** (A) Human thalamic subdivisions as defined by histology and implemented in the MNI152 template brain. Four subgroups of nuclei were categorized by their relative positions. We used 35 nuclei per hemisphere (70 nuclei in total) to obtain the seed time series for functional connectivity analysis. (B) RSFC of the thalamic nuclei anterior ventral (AV), posterior ventral part of ventral lateral (VLpv), medial ventral posterior (VPM), lateral pulvinar (PuL), and centre median (CM) nuclei as representative nuclei for limbic, motor-relay, sensory-relay, associative, and non-specified nuclei groups, respectively. RSFC maps are presented in the sagittal plane view of MNI stereotaxic space. Left and right panels are for the left and right seed masks of thalamic nuclei and their RSFC maps. (C) The matrix representation of group RSFC maps for the regional fractions of significant correlations (FWE-corrected $p < .0007$) between all thalamic nuclei seed masks and other brain regions. The vertical and horizontal indices of the matrix represent thalamic nuclear seed masks and their correlated target locations of FreeSurfer parcellations. A darker-colored cell in the matrix means that there are more significant voxels of RSFC in the region of its horizontal index with the seed mask at its vertical index, compared to those with lighter-colored cells. LH = left hemisphere; RH = right hemisphere.

### 2.4. Functional connectivity analysis

RS FMRI was used to compute resting state functional connectivity (RSFC) between thalamic nuclei and multiple brain regions. We implemented a seed-based correlation method (Biswal et al., 1995). For each subject, the seed time series for thalamic nuclei were obtained by averaging the time series of RS FMRI voxels overlapped with their seed masks as defined in the Thalamus Atlas of the Swiss Federal Institute of Technology (ETH) in Zurich and University of Zurich, Switzerland (Fig. 1A) (Krauth et al., 2010). The mean size of nuclei masks was 303.24 $mm^3$ (7 $mm^3$ for the left paraventricular nucleus at minimum and 1833 $mm^3$ for the right medial pulvinar nucleus at maximum). The Pearson correlation coefficients between the seed time series and the time series of whole brain voxels were calculated and standardized by the Fisher transform. We obtained the RSFC maps of 70 seed masks for each individual subject (2380 RSFC maps for all subjects, in total). Note, the averaged timeseries of thalamic seed masks were extracted prior to the spatial smoothing process, and applied to obtain the correlation maps between those and spatially smoothed EPI data.

For the RSFC maps of each thalamic nuclear seed mask, we performed a one-sample *t*-test to get group RSFC maps for control and mTLE groups to observe the within-group characteristics with the age covariates. We also performed a two-sample t-test to get a group difference map between mTLE and control groups with a covariate for subject age. To test the significance of group statistics for 70 seed masks, we considered the significance level of family-wise error corrected $p$ ($p_{FWE}$) $< 0.05$, and finally determined the practical threshold level at $p_{FWE} < 0.0007$ (~0.05/70 seed masks) by adjusting the number of seed masks to the normal, mTLE group, and group difference maps, considering the number of comparisons. The $p_{FWE} < 0.0007$ is approximately equivalent to uncorrected $p < .01$ with minimum cluster size > 3036 cc by a Monte-Carlo random permutation test (number of iterations = 20,000) in the MNI template space (Cox et al., 2017).

### 2.5. Clinical measures to characterize seizure frequency

The seizure frequency has been implicated as a risk factors for progressive structural and functional brain damage (Sutula et al., 2003). Here we report the number of seizures per month as seizure frequency as a quantitative score of subject disease burden.

### 2.6. Post-hoc analysis

To test whether seizure frequency correlated with thalamic nuclear RSFC with the whole brain, we performed a regression analysis for pairs of thalamic nuclei and their target brain locations, assessing each pair for significant differences in RSFC between the normal and mTLE patient groups. For each thalamic nucleus, the voxels with significant group differences in the group difference maps between mTLE and normal control groups were divided into anatomically segregated clusters (Destrieux et al., 2010). The RSFC features of those clusters were then averaged for the regression analysis with respect to seizure frequency and adjusted for the covariate of age. The final correlation coefficients were thresholded at the significance level of $p_{FWE} < 0.05$, adjusted by the total number of clusters in the group difference map for each seed mask.

### 2.7. Robustness of findings

To observe the robustness of findings for a different preprocessing strategy, we performed the same analyses for the RSFC group comparison and regression analysis with seizure frequency scores by using the global correlation (GCOR) correction method (Gotts et al., 2013; Saad et al., 2013). For the representative seed masks, in addition, we mapped the numbers of individual subjects having significant RSFC at a threshold level $p > .05$ for each group to test the consistency of results across subjects, and also performed the leave-one-out cross validation (LOOCV) for group difference statistics to test whether there are significant outliers that can bias the results.

## 3. Results

### 3.1. RSFC of thalamic nuclei seed masks in normal subjects

RSFCs for the seed masks of representative thalamic nuclei in the control group are presented in Fig. 1-B and -C. Most of the 70 seed masks showed RSFC maps consistent with their previously established main inputs and outputs. For example, the RSFC of the anterior ventral nucleus (AV), posterior ventral part of ventral lateral nucleus (VLpv), medial part of ventral posterior nucleus (VPM), lateral pulvinar nucleus (PuL), and centre median nucleus (CM) showed significant correlations with their target regions, reflecting the main connectivity of limbic, motor relay, sensory relay, associative, and central intralaminar nuclear groups, respectively (Fig. 1B). The RSFCs of all thalamic nuclear seed masks in the normal subjects are summarized in Fig. 1C, and Tables 2 and 3.

### 3.2. Group differences in thalamic RSFC between mTLE and normal subjects

Compared to controls, patients with mTLE showed decreased RSFC for seed masks of the left paraventricular nucleus (Pv) and the magnocellular or limbic portion of the mediodorsal nucleus (MDmc). The most robust difference between controls and mTLE patients was the higher RSFC between the MDmc and the cingulate in the former group (the first row of Fig. 2A). No significant difference was seen among other nuclei in anterior group (anterior dorsal; AD, anterior medial; AM, AV, and lateral dorsal; LD).

In contrast, mTLE patients showed increased RSFC compared to controls in both motor relay ventral anterior VA, and ventral lateral VL nuclei and somatosensory relay (ventral posterior lateral nucleus, VPL) nuclei. Significant differences were found for seed marks of the left parvocellular VL (VLpv), right VLpv (the second row of Fig. 2A), anterior VL (VLa), and the lateral posterior and anterior portions of the VPL (VPLp/VPLa); target regions with significant group differences were all concentrated in the sensory-motor system (the third row of Fig. 2A). Unlike the somatosensory relay nuclei, there was decreased RSFC for seed masks in other sensory relay nuclei, including the left magnocellular lateral geniculate nucleus (LGNmc) and right medial geniculate nucleus (MGN).

The RSFC for seeds in the associative and intralaminar nuclei

**Table 2**
Categorical representations of thalamic nuclear groups. Note the terms "principle input" and "principle output" were derived from priori anatomical knowledge, and not from fMRI analyses alone.

| Functional anatomy | | Principle Input | Principle Output |
|---|---|---|---|
| Group by anatomical connections | Representative nuclei | | |
| Limbic nuclei | AD, AM, AV, MD, LD | Mammillary complex, amygdala, hypothalamus | Cingulate gyrus, prefrontal cortex |
| Motor relay nuclei | VA, VL | Basal ganglia, cerebellum | Premotor cortex, supplementary motor area, primary motor cortex, precentral gyrus |
| Sensory relay nuclei | VPL, VPM, LGN, MGN | Lemniscus, optic tract | Postcentral gyrus, paracentral lobule, postcentral gyrus, cuneus and lingual gyri, superior transverse temporal gyri |
| Association nuclei | Li, LP, Pu | Parietal, prefrontal, occipital cortex | Parietal, prefrontal, occipital cortex |
| Intralarminar nuclei | CeM, CL, CM, Pf, sPf | Brainstem reticular formation | Caudate, putamen, cortex |

showed nucleus and subnucleus-specific differences between the mTLE and control groups. There was increased RSFCs in right limitans nucleus (Li), left and right anterior pulvinar (PuA), medial pulvinar (PuM, shown in the fourth row of Fig. 2A), right lateral pulvinar (PuL) and right lateral posterior nucleus (LP); in contrast, seed masks of inferior pulvinar (PuI) showed decreased RSFC in mTLE compared to controls. Among intralaminar nuclei, mTLE patient had increased connectivity of the left and right centromedian nucleus (CM, shown in the fifth row of Fig. 2A), and decreased connectivity for the central medial nucleus (CeM) and right parafascicular nucleus (Pf).

In summary, nuclei located in the medial part of thalamus (Pv, MDmc, and Pf) except for the CM and the Li, showed decreased RSFC in mTLE patients compared to controls whereas sensory and motor relay nuclei in the lateral group showed increased connectivity with other brain regions. Posterior nuclei, including most subdivisons of the pulvinar showed increased RSFC whereas the inferior pulvinar and geniculate nuclei showed decreased RSFC. The significant RSFC differences between mTLE and control groups were summarized in Fig. 2B and C.

### 3.3. Relationship between thalamic RSFCs and seizure frequency in mTLE group

Of the 25 seed masks that showed significant differences in thalamic RSFC between mTLE and control groups, seizure frequency in mTLE patients as assessed by sezure frequency was highly correlated with differences in RFSC of 16 seed masks compared to controls. (Fig. 3A and B, and Table 4). With respect to the limbic nuclear group, RSFC between the left MDmc and right anterior middle cingulate gyrus and between the right MDmc and the right dorsal posterior cingulate gyrus were negatively correlated with the sezure frequency; while that between the left Pv and left pericallosal sulcus was positively correlated with sezure frequency.

Among the sensory relay nuclei, RSFC between the left VPLp and the right transverse superior temporal sulcus, between the right VPLp and right long insular gyrus/central sulcus of the insula, between the left LGNmc and right hippocampus/parahippocampal gyrus, and between the right MGN and left dorsal posterior cingulate gyrus showed negative correlations with the sezure frequency. In contrast, RSFC between the left VLpv and right lateral superior temporal gyrus, right VLpv and left subcentral gyrus/sulcus, and left VPLa and the right middle temporal gyrus showed positive correlations with sezure frequency.

For the associative nuclei, RSFC between the right Li and right superior parietal gyrus, between the left PuI and left paracentral lobule and sulcus, the right PuL and right superior segment of the circular sulcus of the insula, and between the right PuL and right lateral superior temporal gyrus showed positive correlations with sezure frequency. RSFC between right PuM and right orbital part of the inferior frontal gyrus showed negative correlation with sezure frequency. Finally, among the intralaminar nuclei, RSFC between the left CM and right middle frontal gyrus and between the right CM and right anterior transverse temporal gyrus were negatively correlated with sezure frequency.

### 3.4. Robustness of findings

The RSFC group differences derived from the GCOR method were not much different from those with the ANATICOR method in the group difference maps, and the numbers and peak locations of clusters were quite similar to each other for both methods (see the supplementary Fig. S1). Although the group difference maps of the GCOR method were covering wider areas by expanding the boundaries of the clusters at the same threshold level, there was no significant difference or sign change in the correlation coefficients between the RSFCs and seizure frequencies of the mTLE group for the seeds and target clusters (see the supplementary Fig. S2). For the GCOR method, interestingly, four thalamic seed masks (left limitans; Li, ventral medial; VM, lateral posterior; LP, and suprageniculate; SG nuclei) newly showed the group differences, but there is no significant correlation between their RSFC and seizure frequencies in mTLE group.

The group-based statistical findings results reflect those at the individual subject level as shown by the numbers of subjects having significant RSFC in mTLE and HC (supplementary Fig. S3). The LOOCV results demonstrate the reliability of the spatial patterns of significant group differences, and there is no significantly concentrated variance (high RMSE scores) (supplementary Fig. S4).

## 4. Discussion

This study investigates the resting state functional connectivity of thalamic nuclei with other brain regions including the neocortex and hippocampus in normal and epileptic human brain. Because of the intimate involvement of the thalamus with many neurological processes, thalamic RSFC can yield important insights into fundamental neurophysiology as well as provide a biomarker for neurological disease states. Illustrating this latter point, a number of differences between subjects with mTLE and normal subjects were found, encompassing both increases and decreases in RSFC with various thalamic nuclear groups. The findings and interpretations at the level of thalamic nuclear groups can be summarized as follows.

### 4.1. Limbic nuclei

The limbic system is a functional grouping of brain structures implicated in affective behavior, cognition, and memory that includes regions of neocortex, archicortex and varying subcortical structures (including the hippocampus and parts of the temporal lobe). The limbic nuclei of the thalamus are recognized as major hubs for relaying and processing signals from diverse brain areas involved in limbic function (Child and Benarroch, 2013). With respect to the limbic nuclei, we found decreased RSFC in seed masks for the left Pv and the MDmc with

**Table 3**
Subcortical (indices 1–10) and cortical (indices 11–84) regions parcellated by FreeSurfer software, sorted by alphabetical orders of short names.

| Index | Short name | Long Name | Index | Short name | Long Name |
|---|---|---|---|---|---|
| 1 | Accumbens-area | Accumbens area | 43 | G temp sup G T transv | Anterior transverse temporal gyrus of Heschl |
| 2 | Amygdala | Amygdala | 44 | G temp sup Lateral | Lateral aspect of the superior temporal gyrus |
| 3 | Brain Stem | Brain Stem | 45 | G temp sup Plan polar | Planum polare of the superior temporal gyrus |
| 4 | Caudate | Caudate | 46 | G temp sup Plan tempo | Planum temporale or temporal plane of the superior temporal gyrus |
| 5 | Cerebellum | Cerebellum Cortex | 47 | G temporal inf | Inferior temporal gyrus |
| 6 | Hippocampus | Hippocampus | 48 | G temporal middle | Middle temporal gyrus |
| 7 | Pallidum | Pallidum | 49 | Lat Fis ant Horizont | Horizontal ramus of the anterior segment of the lateral sulcus |
| 8 | Putamen | Putamen | 50 | Lat Fis ant Vertical | Vertical ramus of the anterior segment of the lateral sulcus |
| 9 | Substancia Nigra | Substancia Nigra | 51 | Lat Fis post | Posterior ramus of the lateral sulcus |
| 10 | VentralDC | Ventral Diencephalon | 52 | Pole occipital | Occipital pole |
| 11 | G and S frontomargin | Fronto-marginal gyrus of Wernicke and sulcus | 53 | Pole temporal | Temporal pole |
| 12 | G and S occipital inf | Inferior occipital gyrus and sulcus | 54 | S calcarine | Calcarine sulcus |
| 13 | G and S paracentral | Paracentral lobule and sulcus | 55 | S central | Central sulcus |
| 14 | G and S subcentral | Subcentral gyrus (central operculum) and sulci | 56 | S cingul Marginalis | Marginal branch of the cingulate sulcus |
| 15 | G and S transv frontopol | Transverse frontopolar gyri and sulci | 57 | S circular insula ant | Anterior segment of the circular sulcus of the insula |
| 16 | G and S cingul Ant | Anterior part of the cingulate gyrus and sulcus (ACC) | 58 | S circular insula inf | Inferior segment of the circular sulcus of the insula |
| 17 | G and S cingul Mid Ant | Middle-anterior part of the cingulate gyrus and sulcus (aMCC) | 59 | S circular insula sup | Superior segment of the circular sulcus of the insula |
| 18 | G and S cingul Mid Post | Middle-posterior part of the cingulate gyrus and sulcus (pMCC) | 60 | S collat transv ant | Anterior transverse collateral sulcus |
| 19 | G cingul Post dorsal | Posterior-dorsal part of the cingulate gyrus (dPCC) | 61 | S collat transv post | Posterior transverse collateral sulcus |
| 20 | G cingul Post ventral | Posterior-ventral part of the cingulate gyrus (vPCC, isthmus of the cingulate gyrus) | 62 | S front inf | Inferior frontal sulcus |
| 21 | G cuneus | Cuneus | 63 | S front middle | Middle frontal sulcus |
| 22 | G front inf Opercular | Opercular part of the inferior frontal gyrus | 64 | S front sup | Superior frontal sulcus |
| 23 | G front inf Orbital | Orbital part of the inferior frontal gyrus | 65 | S interm prim Jensen | Sulcus intermedius primus of Jensen |
| 24 | G front inf Triangul | Triangular part of the inferior frontal gyrus | 66 | S intrapariet and P trans | Intraparietal sulcus and transverse parietal sulci |
| 25 | G front middle | Middle frontal gyrus | 67 | S oc middle and Lunatus | Middle occipital sulcus and lunatus sulcus |
| 26 | G front sup | Superior frontal gyrus | 68 | S oc sup and transversal | Superior occipital sulcus and transverse occipital sulcus |
| 27 | G Ins lg and S cent ins | Long insular gyrus and central sulcus of the insula | 69 | S occipital ant | Anterior occipital sulcus and preoccipital notch (temporo-occipital incisure) |
| 28 | G insular short | Short insular gyri | 70 | S oc temp lat | Lateral occipito-temporal sulcus |
| 29 | G occipital middle | Middle occipital gyrus (lateral occipital gyrus) | 71 | S oc temp med and Lingual | Medial occipito-temporal sulcus (collateral sulcus) and lingual sulcus |
| 30 | G occipital sup | Superior occipital gyrus | 72 | S orbital lateral | Lateral orbital sulcus |
| 31 | G oc temp lat fusifor | Lateral occipito-temporal gyrus (fusiform gyrus) | 73 | S orbital med olfact | Medial orbital sulcus (olfactory sulcus) |
| 32 | G oc temp med Lingual | Lingual gyrus, ligual part of the medial occipito-temporal gyrus | 74 | S orbital H Shaped | Orbital sulci (H-shaped sulci) |
| 33 | G oc temp med Parahip | Parahippocampal gyrus, parahippocampal part of the medial occipito-temporal gyrus | 75 | S parieto occipital | Parieto-occipital sulcus |
| 34 | G orbital | Orbital gyri | 76 | S pericallosal | Pericallosal sulcus |
| 35 | G pariet inf Angular | Angular gyrus | 77 | S postcentral | Postcentral sulcus |
| 36 | G pariet inf Supramar | Supramarginal gyrus | 78 | S precentral inf part | Inferior part of the precentral sulcus |
| 37 | G parietal sup | Superior parietal lobule | 79 | S precentral sup part | Superior part of the precentral sulcus |
| 38 | G postcentral | Postcentral gyrus | 80 | S suborbital | Suborbital sulcus (sulcus rostrales, supraorbital sulcus) |
| 39 | G precentral | Precentral gyrus | 81 | S subparietal | Subparietal sulcus |
| 40 | G precuneus | Precuneus | 82 | S temporal inf | Inferior temporal sulcus |
| 41 | G rectus | Straight gyrus, Gyrus rectus | 83 | S temporal sup | Superior temporal sulcus (parallel sulcus) |
| 42 | G subcallosal | Subcallosal area, subcallosal gyrus | 84 | S temporal transverse | Transverse temporal sulcus |

the cingulate regions. Functionally, the MD is mainly involved in maintaining and modulating working memory (Golden et al., 2016; Mitchell and Chakraborty, 2013; Watanabe and Funahashi, 2012), exhibiting topographic projections to the frontal lobe and cingulate cortex (Klein et al., 2010). The medial division is more densely connected with the medial temporal lobes and ventral tegmental area (Mitchell and Chakraborty, 2013), whereas the posterior portion receives highly convergent pathways from the motor regions (Rouiller et al., 1999).

The mediodorsal group of thalamic nuclei has shown strong connectivity to the superior, middle, and inferior frontal gyri, with the

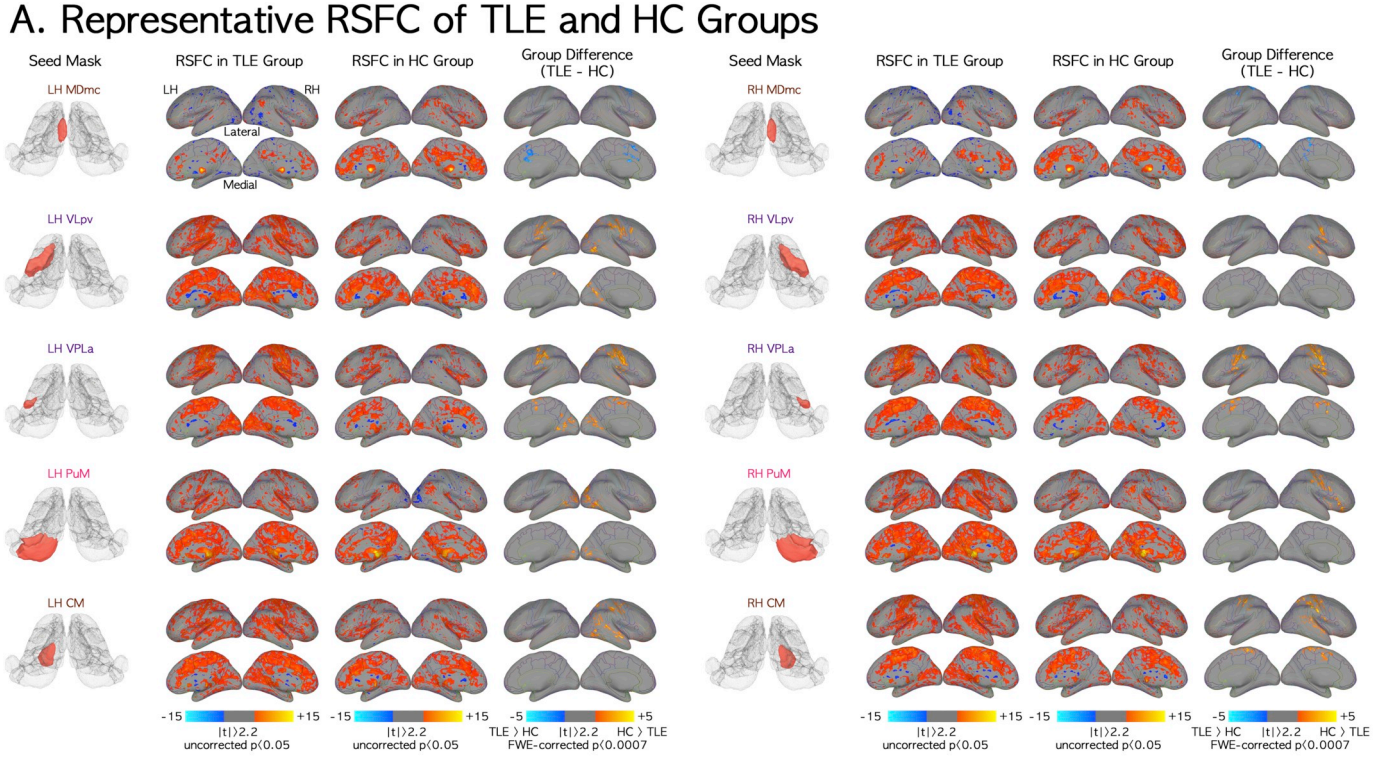


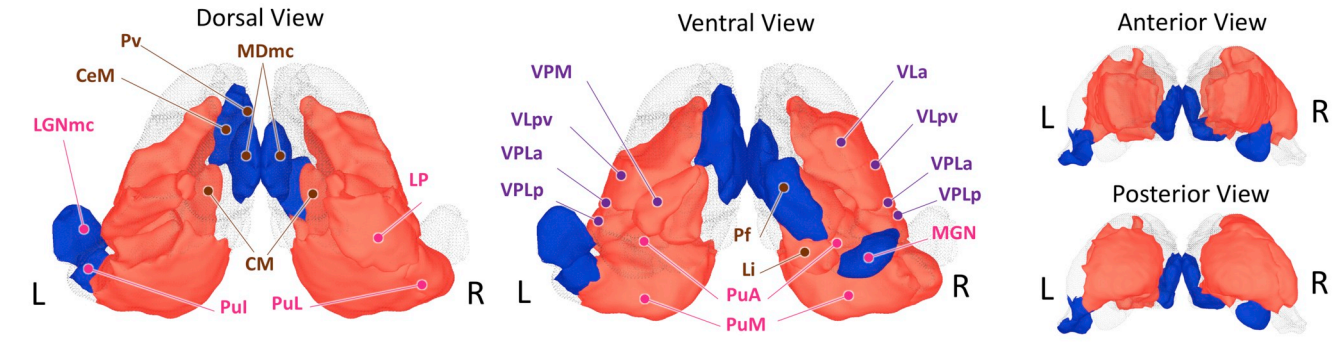


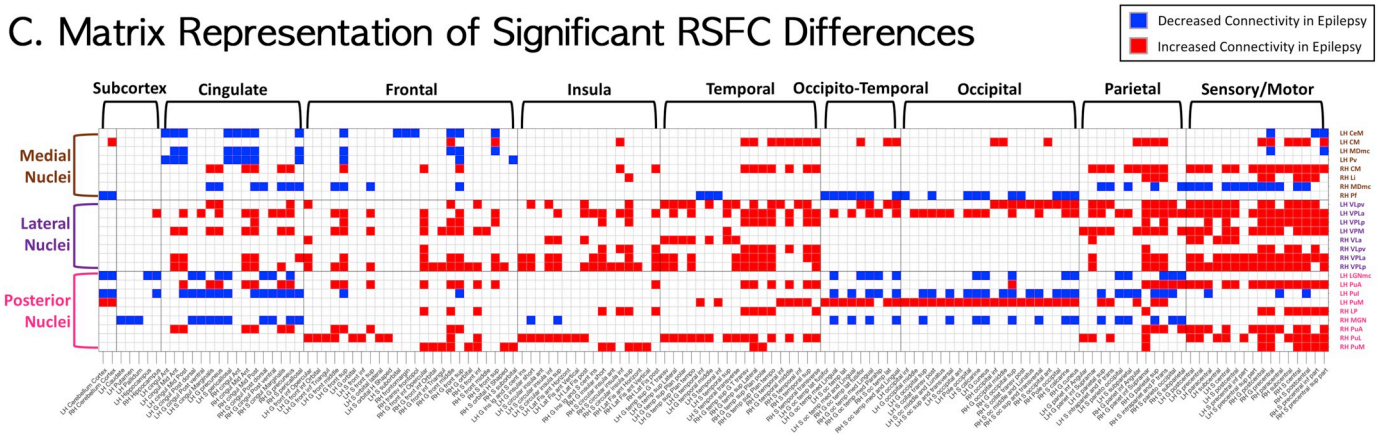


*(caption on next page)*

**Fig. 2.** Significant RSFC differences between mTLE and normal control groups. With respect to group differences in functional connectivity of medial thalamic nuclei group between temporal lobe epilepsy and normal control groups, 8 out of 22 seed masks showed significant differences in RSFC in the temporal lobe epilepsy group as compared to the normal control group (significance level at family-wise-error corrected $p < .05/70 = 0.0007$). (A) The five seed masks, their RSFC for mTLE and normal control groups, and the RSFC difference between the two groups. Magnocellular medial dorsal (MDmc), VLpv, lateral anterior part of ventral posterior lateral (VPLa), medial pulvinar (PuM), and CM seed masks are here representative of RSFC for the limbic, motor-relay, sensory-relay, associative, and non-specified nuclear functional groupings. (B) Seed masks with decreased RSFC (blue) and increased RSFC (red) in the epilepsy group. Nuclei located in the medial part of thalamus generally showed decreased RSFC except CM and limitans (Li) nuclei. All nuclei in the lateral group showed increased connectivity with other brain regions. Posterior nuclei adjacent to those in the lateral group showed increased RSFC, and lateral-end posterior nuclei showed decreased RSFC. The significance level is at family-wise-error corrected $p < .05/70 = 0.0007$. (C) Matrix demonstrating locations of voxels with significant group differences in RSFC for the thalamic nuclear seed masks. RSFC maps for each thalamic nuclear seed mask were thresholded at FWE-corrected $p < .0007$. Vertical and horizontal indices of the matrix stand for the labels at seed masks and parcellated brain regions, respectively. Overall, the RSFC of thalamic nuclei and cingulate, frontal, parietal, and sensory-motor areas in epilepsy group commonly showed significant differences from those in the normal control group. Specifically, in comparison with the control group, the medial nuclei of mTLE subjects showed significant group differences in RSFC with cingulate, frontal, temporal, parietal, and sensory-motor areas while the lateral and posterior nuclei groups showed overall significantly increased RSFC with wide-spread cortical and subcortical regions including the hippocampus. Specific subcortical and cortical regions are listed in Table 3. LH = left hemisphere; RH = right hemisphere. (For interpretation of the references to color in this figure legend, the reader is referred to the web version of this article.)

cingulate gyrus also showing strong connectivity to the mediodorsal group relative to other nuclear groups (Golden et al., 2016). A transition in the connectivity gradient between the anterior region, with projections to the pre-frontal regions, and the posterior region, with projections to the pre-motor and supplementary motor cortices, has been documented (Rouiller et al., 1999). Functionally, the MD is mainly involved in maintaining and modulating working memory (Watanabe and Funahashi, 2012) – exhibiting topographic projections to the frontal lobe and cingulate cortex (Klein et al., 2010). The medial division in particular is more densely connected with the medial temporal lobes and ventral tegmental area (Mitchell and Chakraborty, 2013), whereas the posterior portion receives highly convergent pathways from the motor regions (Rouiller et al., 1999).

There is evidence of a role for the midline thalamus in limbic epilepsy, particularly with respect to the medial dorsal region (Bertram, 2007; Bertram et al., 2001). Studies of the role of the MD in epilepsy have often demonstrated a relative strengthening of the functional connectivity of the MD region with cortical regions relative to controls (Golden et al., 2016), which is consistent with our findings regarding the posterior and lateral portion of this nuclear group. The positive correlation in RSFC between MDmc and cingulate/frontal regions is particularly interesting in this context. It is possible, given the established role that this region plays in memory, that the strengthening of RSFC represents an attempt by the brain to compensate for a disruption of the normal function of this region. This would be consistent with the working memory impairment seen in patients with temporal lobe epilepsy (Campo et al., 2013). Alternatively, the increase in RSFC may be a marker of an abnormality of the involved network, rather than a compensatory mechanism. It is interesting to note that enhanced RSFC in networks involving the mediodorsal thalamus has been observed among patients with the Lennox-Gastaut syndrome (Warren et al., 2017). Previous work by this group has suggested that regions in these networks were recruited early in characteristic seizures among patients with this syndrome (Warren et al., 2016), implying that the increase in RSFC was actually a result of epileptogenic activity being communicated across a shared network. The Pv nucleus, implicated in mood and arousal and stress responses (Hsu et al., 2014), has strong reciprocal connections with the amygdala and other limbic regions (Benarroch, 2015a).

Interestingly, there was no difference in RSFC among the anterior group nuclei in mTLE. Because of its centrality to limbic circuitry and the strong relationship of the limbic system to mTLE, the anterior thalamic nuclear complex (AD, AM, and AV) is a target for therapeutic electrical stimulation for patients with mTLE. While it has been suggested that in an “epileptogenic network” RSFC is increased among the nodes of that network (Bertram et al., 2001), there are a few reasons why nevertheless the RSFC of the anterior nuclear group may have remained normal in mTLE, despite the implicated involvement of the anterior nuclear group in limbic epilepsy and its established efficacy as a DBS target for mTLE (Salanova et al., 2015). It could be that although this group is a useful target for neurostimulation, it is not directly involved in an epileptogenic network per se. Perhaps there is a distinction between nodes involved directly in epileptogenicity and those implicated in propagation. Alternatively, perhaps the anterior nucleus is indeed a node in an epileptogenic network involved in mTLE, but for whatever reason this does not manifest with a change in mTLE.

### 4.2. Sensory-motor relay nuclei

With respect to the motor and sensory relay nuclei, epileptic patients showed increased RSFC for the seed masks of left and right parvocellular ventral lateral nucleus (VLpv), and anterior ventral lateral nucleus (VLa), as well as the VPLp and VPLa, and decreased RSFC for seed masks of left magnocellular lateral geniculate nucleus (LGNmc), and right medial geniculate nucleus (MGN). The VL group had strong cortical connectivity to the primary motor cortex, superior and middle frontal gyri and frontal pole, and subcortically to the striatum and brainstem (Mason et al., 2000). The gradient of connectivity was aligned along an anterior-rostral to posterior-caudal axis. The posterior aspect had greater connectivity to the motor-sensory cortices, mesencephalon, bilateral cerebellum, and brainstem. Anteriorly, VL had greater connectivity to prefrontal regions including the inferior frontal gyri (motor speech areas), with some connectivity to the medial temporal lobe. The posterior VL thalamus forms a major relay circuit between the motor cortex and cerebellum, with lesions situated within the anterior medial portions of VL causing abnormalities in verbal fluency and speech (Schmahmann, 2003). The ventroposterior group is known to have strong connectivity to both the primary motor and sensory cortices, in addition to the superior frontal gyrus, insula, and brainstem (Behrens et al., 2003; Schell and Strick, 1984). In comparison with controls, mTLE patients showed an increase in RSFC between cortex and nuclei of the lateral group with the exception of the VA group. This may represent portions of an underlying epileptogenic network in the mTLE patients, perhaps pertaining to the semiology of temporal lobe epilepsy (often characterized by sensory phenomena and stereotyped automatisms, the latter likely representing either release or stimulation of motor programs) (Mirzadjanova et al., 2010; Unnwongse et al., 2009).

Findings with respect to seizure frequency were complex, with variable effects (and variable lateralization of those effects) among nuclei. The LG group is a known relay in the visual system, receiving afferents from the optic tract and projecting to the visual cortices via the optic radiation (Burgel et al., 1999). In contrast, the MG region is the primary relay for all ascending auditory information, projecting on to cortical auditory processing areas (Winer et al., 1999). The left-sided decrease in RSFC with respect to the LG and the right-sided decrease in RSFC of the MG are of unclear significance, particularly given the relative paucity of left-handed patients among our cohort.

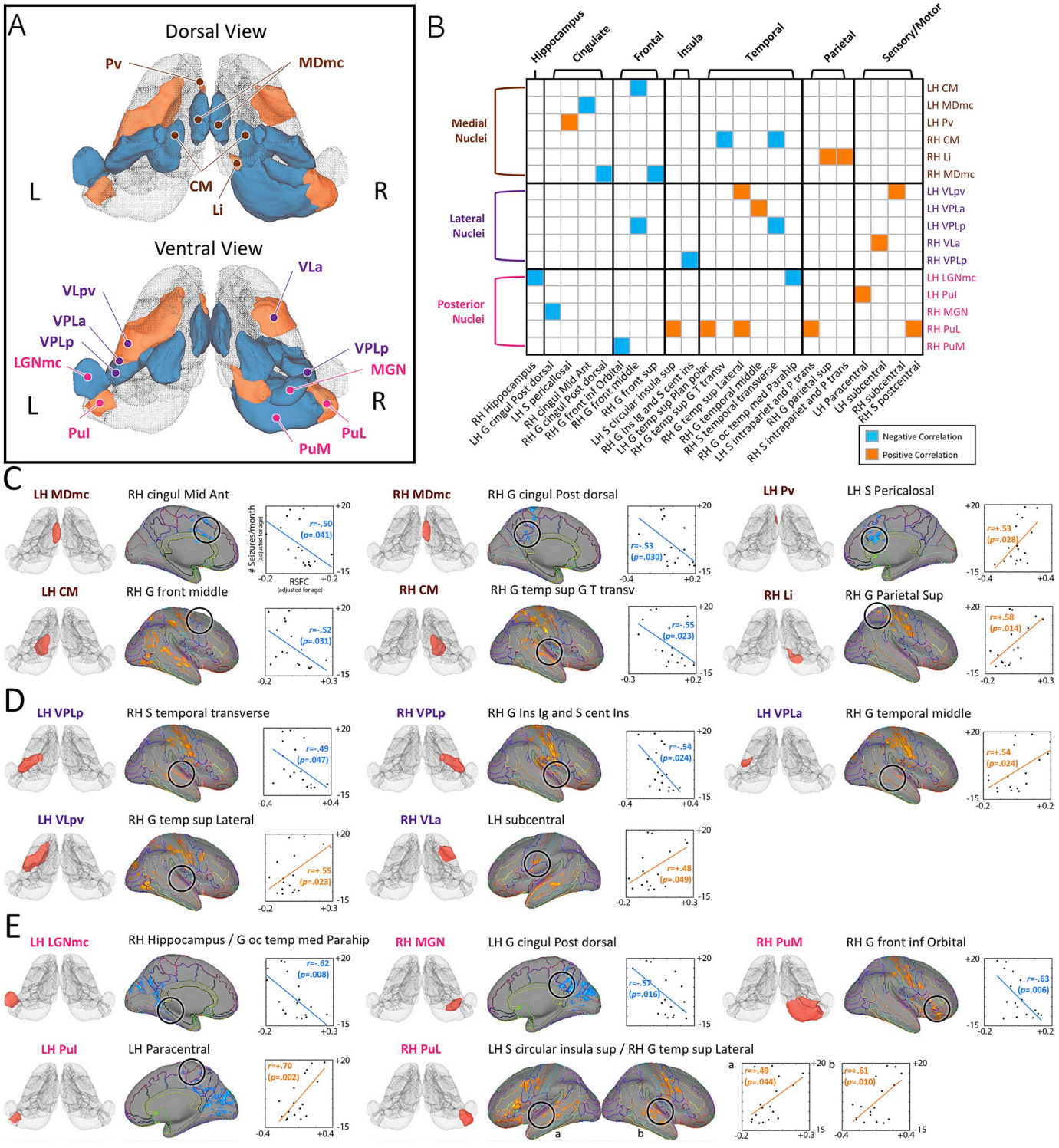


**Fig. 3.** Magnitude of RSFC between thalamic nuclei and other brain regions in mTLE patients predicts the seizure frequency. Candidates for regression analysis with regards to RSFC were chosen among those nuclei with significant group difference between epilepsy and normal control groups (25 nuclei; see Fig. 2C for details). For each thalamic nucleus, those voxels with a significance level of FWE-corrected $p < .0007$ for group statistics between epilepsy and normal control groups were divided into anatomically distinguished clusters (Destrieux et al., 2010). The RSFC in those clusters was then averaged for the regression analysis. The correlation coefficients were thresholded at the significance level of FWE-corrected $p < .05$. (A) 16 thalamic nuclei showed relatively higher correlations between seizure frequency and their RSFC with other brain regions. The nuclei shown here in orange had positive correlation between RSFC and seizure frequency while those in light blue had negative correlation between RSFC and seizure frequency. (B) Matrix showing locations of clusters with significant correlation between RSFC and seizure frequency for thalamic nuclear seed masks. The RSFCs showing significant correlation with seizure frequency are presented in (C), (D), and (F) for the medial, lateral, and the posterior nuclear groups, respectively. Thalamic nuclei and associated brain regions are listed in Fig. 1A and Table 3, respectively. (For interpretation of the references to color in this figure legend, the reader is referred to the web version of this article.)

**Table 4**
Summary of findings for significant thalamic RSFC differences between normal *and* TLE groups. The correlations between thalamic nuclear RSFCs in TLE subjects and their seizure frequency are also presented with their target locations. The long names of thalamic nuclei and target locations are presented in Fig. 1A and Table 3, respectively. Target locations of major functional anatomy connections for seed masks were presented in the **bold** fonts.

| Seed mask for RSFC | | | | | RSFC difference in TLE, compared to the normal group | | Target location correlated with seizure frequency ($p_{FWE\text{-}corrected} < 0.05$) | |
|---|---|---|---|---|---|---|---|---|
| Group by functional anatomy | Group by relative position | Thalamic nucleus | Principle input | Principle Output | For LH seed | For RH seed | For LH seed | For RH seed |
| Limbic | Medial | MDmc | Limbic system, prefrontal cortex, orbitofrontal cortex | Limbic system, orbitofrontal cortex | Decreased | Decreased | **RH cingul Mid Ant** | **RH G cingul Post dorsal** |
| | | Pv | Limbic system, hypothalamus | Limbic system | Decreased | None | S Pericalosal | |
| Motor relay | Lateral | VLa | Cerebellum (dentate nucleus), basal ganglia | Primary motor cortex, premotor cortex | None | Increased | | **LH subcentral** |
| | | VLpv | Cerebellum (dentate nucleus), basal ganglia | Primary motor cortex, premotor cortex | Increased | Increased | RH G temp sup Lateral | |
| Sensory relay | Lateral | VPLa | Spinothalamic tract, medial lemniscus | Postcentral gyrus | Increased | Increased | RH G temporal middle | |
| | | VPLp | Spinothalamic tract, medial lemniscus | Postcentral gyrus | Increased | Increased | RH S temporal transverse | RH G Ins lg and S cent Ins |
| | | VPM | Trigeminothalamic tracts | Postcentral gyrus | Increased | None | | |
| | Posterior | LGNmc | Retinal ganglion cells | Primary visual cortex | Decreased | None | RH Hippocampus/G oc temp med Parahip | |
| | | MGN | Inferior colliculus, others | Auditory cortex | None | Decreased | | LH G cingul Post dorsal |
| Association | Medial | Li | Superior colliculus, auditory cortex | Association cortex | None | Increased | | RH G Parietal Sup |
| | Posterior | LP | association cortex, primary and higher visual cortices, anterior cingulate cortex, superior colliculus | All visual areas, telencephalic structures | None | Increased | | |
| | | PuA | Somatosensory cortex | Somatosensory cortex, association cortex | Increased | Increased | | |
| | | PuI | Association cortex, subcortical regions | Association cortex | Decreased | None | LH paracentral | |
| | | PuL | Association cortex, subcortical regions | Association cortex | None | Increased | | LH S circular insula sup<br>RH G temp sup Lateral |
| | | PuM | Association cortex, subcortical regior | Association cortex | Increased | Increased | | RH G front inf Orbital |
| Intralaminary | Medial | CeM | Basal ganglia, brainstem | Diffuse (cortex, basal ganglia) | Decreased | None | | |
| | | CM | Reticular activating system | Diffuse (cortex, basal ganglia) | Increased | Increased | RH G front middle | RH G temp sup G T transv |
| | | Pf | Reticular activating system, sensory inputs | Diffuse (cortex, basal ganglia) | None | Decreased | | |

### 4.3. Associative nuclei

Among the associative nuclei, increased connectivity for mTLE patients was observed in the right Li, right LP, bilateral PuA and PuM and right PuL. mTLE patients showed decreased RSFC for seed masks inferior pulvinar (PuI). The pulvinar nucleus is the largest thalamic nuclear mass in the thalamus. Its connections include somatosensory cortex (PuA), visual cortex, limbic areas, multimodal association cortex and subcortical regions (Benarroch, 2015b). Regions of the pulvinar contain retinotopic representations of the visual field and, among its association functions, the pulvinar is thought to play roles in visual attention and face processing. There is ample evidence for a relationship between the pulvinar and mTLE, via electrophysiology and imaging (Chatzikonstantinou et al., 2011; Rosenberg et al., 2006), consistent with its established connections with the hippocampus and temporal lobe (Benarroch, 2015b). The implication of the pulvinar among our mTLE cohort is unsurprising in this context.

### 4.4. Intralarminar nuclei

Among the central intralarminar thalamic nuclei, epileptic patients showed decreased connectivity for central medial nucleus (CeM), and right parafascicular nucleus (Pf) seeds, while increased connectivity for mTLE patients was observed for the seed masks of the left and right CM. The CM and Pf have been known to have a broad pattern of connectivity to the orbitofrontal, enterorhinal and calcarine cortices, and subcortically to the striatum, amygdala and ventral mescencephalon. These nuclei are known to receive extensive inputs from the upper brainstem neuromodulatory nuclei (Pare et al., 1988), reciprocally connect the medial temporal lobe and prefrontal cortex (Saalmann, 2014), and are proposed to modulate memory networks. The CM is a target for DBS in epilepsy (Velasco et al., 1987), particularly in the case of the refractory generalized epilepsies. The findings regarding increased RSFC among patients with mTLE are therefore particularly compelling. Further study should seek to determine whether the increase in RSFC is more pronounced among patients with generalized epilepsy or with a focal epilepsy with a tendency toward generalization.

### 4.5. Limitations of the study and technical issues

Several limitations and technical issues are pertinent to this study. First, this study is based on a small sample size. Therefore, these results should be interpreted with caution, particularly regarding the possibility of planning targeted interventions, since it is possible that some of the findings may not generalize to the broader population with temporal lobe epilepsy. Second, the seed masks of thalamic nuclei have different numbers of voxels, and the averaged timeseries within those can have different signal-to-noise ratios. One possible suggestion might be the ROI parcellation that divides the thalamic areas into multiple clusters with similar voxel numbers, but this method also might lead ambiguous interpretations for those laid on the anatomical boundaries in the thalamus. Third, atrophy and imaging suggestive of sclerosis were found in the structural MRI data for 3 patients.[1] However, we could not adjust the fMRI data to correct for atrophy and/or sclerosis in partial samples in one group while performing a two-sample *t*-test for two groups. It is to be hoped that this methodological dilemma will be tractable to future investigations in data collection and analysis, as it represents a salient problem for not only epilepsy but also the broader field of neurological imaging.

[1] Aside from the visual inspection to assess thalamic atrophy, recent studies using quantitative MRI analyses have reported global as well as segmental thalamic atrophy in TLE (seeBonilha and Keller, 2015for review).

## Acknowledgment

This study was supported by National Institutes of Health (R01 NS092882, UH2-NS95495) and European Regional Development Fund – Project FNUSA – ICRC (CZ.1.05/1.1.00/02.0123). The Thalamus Atlas is copyrighted by © University of Zurich and ETH Zurich, Axel Krauth, Rémi Blanc, Alejandra Poveda, Daniel Jeanmonod, Anne Morel, Gábor Székely. We thank Dr. Sung Jun Jung and Dr. Gang Chen for helpful discussion on the interpretation of results, and the Mayo High Performance Research Computing Facility (RCF) at Mayo Clinic in Rochester, MN, for providing computational resources.

## Appendix A. Supplementary data

Supplementary data to this article can be found online at https://doi.org/10.1016/j.nicl.2019.101671.

## References

Barron, D.S., Tandon, N., Lancaster, J.L., Fox, P.T., 2014. Thalamic structural connectivity in medial temporal lobe epilepsy. Epilepsia 55, e50–e55.
Barron, D.S., Fox, P.T., Pardoe, H., Lancaster, J., Price, L.R., Blackmon, K., Berry, K., Cavazos, J.E., Kuzniecky, R., Devinsky, O., Thesen, T., 2015. Thalamic functional connectivity predicts seizure laterality in individual TLE patients: application of a biomarker development strategy. Neuroimage Clin. 7, 273–280.
Battistella, G., Najdenovska, E., Maeder, P., Ghazaleh, N., Daducci, A., Thiran, J.-P., Jacquemont, S., Tuleasca, C., Levivier, M., Bach Cuadra, M., Fornari, E., 2017. Robust thalamic nuclei segmentation method based on local diffusion magnetic resonance properties. Brain Struct. Funct. 222, 2203–2216.
Beall, E.B., 2010. Adaptive cyclic physiologic noise modeling and correction in functional MRI. J. Neurosci. Methods 187, 216–228.
Behrens, T.E., Johansen-Berg, H., Woolrich, M.W., Smith, S.M., Wheeler-Kingshott, C.A., Boulby, P.A., Barker, G.J., Sillery, E.L., Sheehan, K., Ciccarelli, O., Thompson, A.J., Brady, J.M., Matthews, P.M., 2003. Non-invasive mapping of connections between human thalamus and cortex using diffusion imaging. Nat. Neurosci. 6, 750–757.
Benarroch, E.E., 2015a. The amygdala: functional organization and involvement in neurologic disorders. Neurology 84, 313–324.
Benarroch, E.E., 2015b. Pulvinar: associative role in cortical function and clinical correlations. Neurology 84, 738–747.
Bergey, G.K., Morrell, M.J., Mizrahi, E.M., Goldman, A., King-Stephens, D., Nair, D., Srinivasan, S., Jobst, B., Gross, R.E., Shields, D.C., Barkley, G., Salanova, V., Olejniczak, P., Cole, A., Cash, S.S., Noe, K., Wharen, R., Worrell, G., Murro, A.M., Edwards, J., Duchowny, M., Spencer, D., Smith, M., Geller, E., Gwinn, R., Skidmore, C., Eisenschenk, S., Berg, M., Heck, C., Van Ness, P., Fountain, N., Rutecki, P., Massey, A., O'Donovan, C., Labar, D., Duckrow, R.B., Hirsch, L.J., Courtney, T., Sun, F.T., Seale, C.G., 2015. Long-term treatment with responsive brain stimulation in adults with refractory partial seizures. Neurology 84, 810–817.
Bertram, E., 2007. The relevance of kindling for human epilepsy. Epilepsia 48 (Suppl. 2), 65–74.
Bertram, E.H., Mangan, P.S., Zhang, D., Scott, C.A., Williamson, J.M., 2001. The midline thalamus: alterations and a potential role in limbic epilepsy. Epilepsia 42, 967–978.
Biswal, B., Yetkin, F.Z., Haughton, V.M., Hyde, J.S., 1995. Functional connectivity in the motor cortex of resting human brain using echo-planar MRI. Magn. Reson. Med. 34, 537–541.
Bonilha, L., Keller, S.S., 2015. Quantitative MRI in refractory temporal lobe epilepsy: relationship with surgical outcomes. Quant. Imaging Med. Surg. 5, 204–224.
Boon, P., Vonck, K., De Herdt, V., Van Dycke, A., Goethals, M., Goossens, L., Van Zandijcke, M., De Smedt, T., Dewaele, I., Achten, R., Wadman, W., Dewaele, F., Caemaert, J., Van Roost, D., 2007. Deep brain stimulation in patients with refractory temporal lobe epilepsy. Epilepsia 48, 1551–1560.
Burgel, U., Schormann, T., Schleicher, A., Zilles, K., 1999. Mapping of histologically identified long fiber tracts in human cerebral hemispheres to the MRI volume of a reference brain: position and spatial variability of the optic radiation. NeuroImage 10, 489–499.
Campo, P., Garrido, M.I., Moran, R.J., Garcia-Morales, I., Poch, C., Toledano, R., Gil-Nagel, A., Dolan, R.J., Friston, K.J., 2013. Network reconfiguration and working memory impairment in mesial temporal lobe epilepsy. NeuroImage 72, 48–54.
Chatzikonstantinou, A., Gass, A., Forster, A., Hennerici, M.G., Szabo, K., 2011. Features of acute DWI abnormalities related to status epilepticus. Epilepsy Res. 97, 45–51.
Child, N.D., Benarroch, E.E., 2013. Anterior nucleus of the thalamus: functional organization and clinical implications. Neurology 81, 1869–1876.
Cox, R.W., 1996. AFNI: software for analysis and visualization of functional magnetic resonance neuroimages. Comput. Biomed. Res. 29, 162–173.
Cox, R.W., Chen, G., Glen, D.R., Reynolds, R.C., Taylor, P.A., 2017. fMRI clustering and false-positive rates. Proc. Natl. Acad. Sci. U. S. A. 114, E3370–E3371.
Cukiert, A., Cukiert, C.M., Burattini, J.A., Mariani, P.P., Bezerra, D.F., 2017. Seizure outcome after hippocampal deep brain stimulation in patients with refractory temporal lobe epilepsy: a prospective, controlled, randomized, double-blind study. Epilepsia 58, 1728–1733.
den Heijer, J.M., Otte, W.M., van Diessen, E., van Campen, J.S., Lorraine Hompe, E.,

Jansen, F.E., Joels, M., Braun, K.P.J., Sander, J.W., Zijlmans, M., 2018. The relation between cortisol and functional connectivity in people with and without stress-sensitive epilepsy. Epilepsia 59, 179–189.
Destrieux, C., Fischl, B., Dale, A., Halgren, E., 2010. Automatic parcellation of human cortical gyri and sulci using standard anatomical nomenclature. NeuroImage 53, 1–15.
Gill, R.S., Mirsattari, S.M., Leung, L.S., 2017. Resting state functional network disruptions in a kainic acid model of temporal lobe epilepsy. Neuroimage Clin. 13, 70–81.
Gloor, P., Olivier, A., Quesney, L.F., Andermann, F., Horowitz, S., 1982. The role of the limbic system in experiential phenomena of temporal lobe epilepsy. Ann. Neurol. 12, 129–144.
Golden, E.C., Graff-Radford, J., Jones, D.T., Benarroch, E.E., 2016. Mediodorsal nucleus and its multiple cognitive functions. Neurology 87, 2161–2168.
Gotts, S.J., Saad, Z.S., Jo, H.J., Wallace, G.L., Cox, R.W., Martin, A., 2013. The perils of global signal regression for group comparisons: a case study of Autism Spectrum Disorders. Front. Hum. Neurosci. 7.
Hsu, D.T., Kirouac, G.J., Zubieta, J.K., Bhatnagar, S., 2014. Contributions of the paraventricular thalamic nucleus in the regulation of stress, motivation, and mood. Front. Behav. Neurosci. 8, 73.
Jo, H.J., Saad, Z.S., Simmons, W.K., Milbury, L.A., Cox, R.W., 2010. Mapping sources of correlation in resting state FMRI, with artifact detection and removal. NeuroImage 52, 571–582.
Jo, H.J., Gotts, S.J., Reynolds, R.C., Bandettini, P.A., Martin, A., Cox, R.W., Saad, Z.S., 2013. Effective preprocessing procedures virtually eliminate distance-dependent motion artifacts in resting state FMRI. J. Appl. Math. 2013, 935154.
Jones, E.G., 2007. The Thalamus, 2nd ed. Cambridge University Press, Cambridge; New York.
Klein, J.C., Rushworth, M.F., Behrens, T.E., Mackay, C.E., de Crespigny, A.J., D'Arceuil, H., Johansen-Berg, H., 2010. Topography of connections between human prefrontal cortex and mediodorsal thalamus studied with diffusion tractography. NeuroImage 51, 555–564.
Krauth, A., Blanc, R., Poveda, A., Jeanmonod, D., Morel, A., Szekely, G., 2010. A mean three-dimensional atlas of the human thalamus: generation from multiple histological data. NeuroImage 49, 2053–2062.
Kumar, V.J., van Oort, E., Scheffler, K., Beckmann, C.F., Grodd, W., 2017. Functional anatomy of the human thalamus at rest. NeuroImage 147, 678–691.
Kwan, P., Brodie, M.J., 2000. Early identification of refractory epilepsy. N. Engl. J. Med. 342, 314–319.
Lambert, C., Simon, H., Colman, J., Barrick, T.R., 2017. Defining thalamic nuclei and topographic connectivity gradients in vivo. NeuroImage 158, 466–479.
Mason, A., Ilinsky, I.A., Maldonado, S., Kultas-Ilinsky, K., 2000. Thalamic terminal fields of individual axons from the ventral part of the dentate nucleus of the cerebellum in Macaca mulatta. J. Comp. Neurol. 421, 412–428.
Mirzadjanova, Z., Peters, A.S., Remi, J., Bilgin, C., Silva Cunha, J.P., Noachtar, S., 2010. Significance of lateralization of upper limb automatisms in temporal lobe epilepsy: a quantitative movement analysis. Epilepsia 51, 2140–2146.
Mitchell, A.S., Chakraborty, S., 2013. What does the mediodorsal thalamus do? Front. Syst. Neurosci. 7, 37.
Pare, D., Smith, Y., Parent, A., Steriade, M., 1988. Projections of brainstem core cholinergic and non-cholinergic neurons of cat to intralaminar and reticular thalamic nuclei. Neuroscience 25, 69–86.
Rosenberg, D.S., Mauguiere, F., Demarquay, G., Ryvlin, P., Isnard, J., Fischer, C., Guenot, M., Magnin, M., 2006. Involvement of medial pulvinar thalamic nucleus in human temporal lobe seizures. Epilepsia 47, 98–107.
Rouiller, E.M., Tanne, J., Moret, V., Boussaoud, D., 1999. Origin of thalamic inputs to the primary, premotor, and supplementary motor cortical areas and to area 46 in macaque monkeys: a multiple retrograde tracing study. J. Comp. Neurol. 409, 131–152.
Saad, Z.S., Reynolds, R.C., Jo, H.J., Gotts, S.J., Chen, G., Martin, A., Cox, R.W., 2013. Correcting brain-wide correlation differences in resting-state FMRI. Brain Connect. 3, 339–352.
Saalmann, Y.B., 2014. Intralaminar and medial thalamic influence on cortical synchrony, information transmission and cognition. Front. Syst. Neurosci. 8, 83.
Salanova, V., Witt, T., Worth, R., Henry, T.R., Gross, R.E., Nazzaro, J.M., Labar, D., Sperling, M.R., Sharan, A., Sandok, E., Handforth, A., Stern, J.M., Chung, S., Henderson, J.M., French, J., Baltuch, G., Rosenfeld, W.E., Garcia, P., Barbaro, N.M., Fountain, N.B., Elias, W.J., Goodman, R.R., Pollard, J.R., Troster, A.I., Irwin, C.P., Lambrecht, K., Graves, N., Fisher, R., Group, S.S, 2015. Long-term efficacy and safety of thalamic stimulation for drug-resistant partial epilepsy. Neurology 84, 1017–1025.
Schell, G.R., Strick, P.L., 1984. The origin of thalamic inputs to the arcuate premotor and supplementary motor areas. J. Neurosci. 4, 539–560.
Schmahmann, J.D., 2003. Vascular syndromes of the thalamus. Stroke 34, 2264–2278.
Sutula, T.P., Hagen, J., Pitkanen, A., 2003. Do epileptic seizures damage the brain? Curr. Opin. Neurol. 16, 189–195.
Tasker, R.R., Organ, L.W., Hawrylyshyn, P.A., 1982. The Thalamus and Midbrain of Man: A Physiological Atlas Using Electrical Stimulation. C.C. Thomas, Springfield, Ill.
Unnwongse, K., Lachhwani, D., Tang-Wai, R., Matley, K., O'Connor, T., Nair, D., Bingaman, W., Wyllie, E., Diehl, B., 2009. Oral automatisms induced by stimulation of the mesial frontal cortex. Epilepsia 50, 1620–1623.
Velasco, F., Velasco, M., Ogarrio, C., Fanghanel, G., 1987. Electrical stimulation of the centromedian thalamic nucleus in the treatment of convulsive seizures: a preliminary report. Epilepsia 28, 421–430.
Warren, A.E., Abbott, D.F., Vaughan, D.N., Jackson, G.D., Archer, J.S., 2016. Abnormal cognitive network interactions in Lennox-Gastaut syndrome: a potential mechanism of epileptic encephalopathy. Epilepsia 57, 812–822.
Warren, A.E.L., Abbott, D.F., Jackson, G.D., Archer, J.S., 2017. Thalamocortical functional connectivity in Lennox-Gastaut syndrome is abnormally enhanced in executive-control and default-mode networks. Epilepsia 58, 2085–2097.
Watanabe, Y., Funahashi, S., 2012. Thalamic mediodorsal nucleus and working memory. Neurosci. Biobehav. Rev. 36, 134–142.
Wiebe, S., Blume, W.T., Girvin, J.P., Eliasziw, M., Effectiveness, Efficiency of Surgery for Temporal Lobe Epilepsy Study, G, 2001. A randomized, controlled trial of surgery for temporal-lobe epilepsy. N. Engl. J. Med. 345, 311–318.
Winer, J.A., Larue, D.T., Huang, C.L., 1999. Two systems of giant axon terminals in the cat medial geniculate body: convergence of cortical and GABAergic inputs. J. Comp. Neurol. 413, 181–197.
Zhang, S., Li, C.-S.R., 2017. Functional connectivity parcellation of the human thalamus by independent component analysis. Brain Connect. 7, 602–616.